Bearing Capacity Analysis of Piled Raft Foundation for Dhaka – Chittagong Elevated Expressway

Ahmed Tohameem Alam

Mehedi Hasan Siddiquee

ISLAMIC UNIVERSITY OF TECHNOLOGY

2017

Bearing Capacity Analysis of Piled Raft Foundation for Dhaka – Chittagong Elevated Expressway

Ahmed Tohameem Alam

Mehedi Hasan Siddiquee

(135433)

(125417)

A THESIS SUBMITTED FOR THE DEGREE OF BACHELOR OF SCIENCE IN CIVIL ENGINEERING
DEPARTMENT OF CIVIL AND ENVIRONMENTAL ENGINEERING

ISLAMIC UNIVERSITY OF TECHNOLOGY

2017

PROJECT REPORT APPROVAL

The thesis titled “Bearing Capacity Analysis of Piled Raft Foundation for Dhaka - Chittagong Elevated Expressway” submitted by Ahmed Tohameem Alam, St. No. 135433 and Mehedi Hasan Siddiquee 125417 has been found as satisfactory and accepted as partial fulfillment of the requirement for the Degree Bachelor of Science in Civil Engineering.

SUPERVISOR

Dr. Hossain MD. Shahin
Professor
Department of Civil and Environment Engineering (CEE)
Islamic University of Technology (IUT)
Board Bazar, Gazipur, Bangladesh

DECLARATION OF CANDIDATE

We hereby declare that the undergraduate research work reported in this thesis has been performed by us under the supervision of Professor Dr. Hossain MD. Shahin and this work has not been submitted elsewhere for any purpose (except for publication).

Dr. Hossain MD. Shahin
Professor
Department of Civil and Environmental Engineering (CEE)
Islamic University of Technology (IUT)
Board Bazar, Gazipur, Bangladesh
Date:

Ahmed Tohameem Alam
Student No: 135433
Academic Year: 2016-2017
Date: /11/2017

Mehedi Hasan Siddiquee
Student No: 125417
Academic Year: 2016-2017
Date: /11/2017

DEDICATION

We dedicate our thesis work to our family. A special feeling of gratitude to our loving parents.

We also dedicate this thesis to our many friends who have supported us throughout the process. We will always appreciate all they have done.

ACKNOWLEDGEMENTS

"In the name of Allah, Most Gracious, Most Merciful"

All the praises to Allah (SWT) for giving us the opportunity to complete this book.

We wish to express our sincere gratitude to Professor Dr. Hossain MD. Shahin for providing us with all the necessary facilities, giving undivided attention and fostering us all the way through the research. His useful comments, remarks and engagement helped us with the learning process throughout the thesis. We want to wish our heartiest gratitude and thanks to 'Noor-Zaman Engineering Foundation' and 'SMEC International Pty Ltd' for their helping hand to us for performing field level soil investigation and collection soil sample from different depths in soil layers from selected places. We would like express gratitude to all of the departmental faculty members for their help and support. We are also grateful to our parents for their encouragement, support and attention and for being ravished patrons.

We want to wish our heartiest gratitude and thanks to our batchmate Mozaher UL Kabir (135427) for helping us with our research works.

TABLE OF CONTENTS

TABLE OF CONTENTS

CHAPTER 3 METHODOLOGY

CHAPTER 6 CONCLUSION

ABSTRACT

Bearing capacity is one of the most important characteristics of any kind of soil. For every construction work it is compulsory to calculate the bearing capacity of soil of study area for particular type of foundation. Bearing capacity is generally calculated by some conventional equations like Terzaghi's bearing capacity equation and Meyerhof's bearing capacity equation and for different types footings these equations vary. In this research extended sub-loading tij model for Finite Element Method (FEM) is used to calculate the bearing capacity of piled raft foundation. Elasto-plastic constitutive model parameter identification is an important task for proper modeling of any soil. In this research, subsoil characteristics of study locations are presented based on field and laboratory test results. Elasto-plastic constitutive model parameters of study locations soil has been determined for extended sub-loading tij model. In this study some soil parameters are determined from laboratory tests and by using these, simulation parameters like Compression index for FEM tij simulation (λ), Swelling index for FEM tij simulation (Ќ), Critical stress ration (RCs) and Void ratio at 98KPa (N) are calculated. Using these parameters, bearing capacity of piled raft foundation has been estimated for 0.05% settlement of soil section. Considering the effect of settlement in 2D Finite Element analysis have been conducted. It is found that bearing capacity determined.

Keywords: Constitutive Model, Bearing Capacity, Settlement, Finite Element *by the conventional methods match well with the results of the numerical simulations.* Method etc.

LIST OF SYMBOLS

Cc	**Compression index**
Cs	**Swelling index**
eo	**Initial void ratio**
LL	**liquid limit**
PL	**Plastic limit**
PI	**Plasticity index**
Wn	**Natural water content**
Gs	**Specific gravity**
GT	**Specific gravity at T0 C**
Δe	**Variation of void ratio**
Δlogσ'	**Variation of effective stress**
Ws	**Weight of dry soil**
V	**Volume of soil sample**
Pc	**Preconsolidation pressure**
qu	**Ultimate compression stress**
σ	**Stress**
€	**Strain**
λ	**Compression index for FEM*tij* simulation**
Ќ	**Swelling index for FEM *tij* simulation**
Rcs	**critical stress ratio**
N	**void ratio at 98kpa**

LIST OF FIGURES

LIST OF TABLES

Chapter 1 Introduction

1.1 General

Bearing capacity is estimated by limit analysis using upper bound and lower bound theory. But the limit state analysis cannot consider the effect of Over Consolidation Ratio (OCR), bonding effect of soil. Therefore, in estimation of bearing capacity such parameters should be considered. A now-a-days FE method is widely used in different fields of Geotechnical Engineering. So, such condition can also be applied for bearing capacity estimation. However, the accuracy of the FE analysis depends on the constitutive models of soils. Available constitutive models such as Camclay model (Roscoe and Burland, 1968), Drucker-Prager Model, Mohr-Coloumb Model cannot properly consider or explain soil behavior of different densities. However, in this paper extended sub-loading *tij* model (Nakai and Hinokio, 2004; Nakai et al., 2011) is used which can consider influence of intermediate principal stress on the deformation and strength of soils, dependence of the direction of plastic flow on the stress paths, influence of density and/or confining pressure and bonding effect on the deformation and strength of soils (Shahin et al,. 2004; Nakai et al., 2010; Nakai et al., 2011).

Pile foundation is a popular deep foundation type used to transfer superstructure load into subsoil and bearing layers. However, accurate prediction of piles' settlement is particularly difficult concerning complicated consolidation process and pile-soil interaction. (Kazimierz, 2015) Piles are commonly used to transfer superstructure load into subsoil and a stiff bearing layer. As it was emphasized by (Lambe and Whitman, 1969), a pile foundation, even in the case of single pile, is statically indeterminate to a very high degree.

The present study is limited to sub-soil properties parameters for constitutive modeling of the ground where the proposed Dhaka-Chittagong elevated Expressway will be constructed.

The main objectives of the study are:

1. Determination of load bearing capacity of piled raft foundation.

1.2 Objectives of the study

- To calculate load bearing capacity of piled raft foundation
- Compare Load Bearing Capacity of Different Lengths of Pile raft
- Establish relationship between load bearing capacity and length of piles

1.3 Scope of the study

1. CALCULATION OF ULTIMATE BEARING CAPACITY OF PILED RAFT FOUNDATION AND PILE FOUNDATION VARYING-

- NUMBER OF PILES
- DIAMETER OF PILES
- CHANGING THE HEIGHT OF THE WATER TABLE

Chapter 2 Literature Review

2.1 General

Literature review has been done to identify the so far studies related to this field. Literature review for our research is load bearing capacity of piled raft foundation.

2.1.1 Load bearing capacity of piled raft foundation

Bearing capacity is estimated by limit analysis using upper bound and lower bound theory. Therefore, in estimation of bearing capacity such parameters should be considered. Now-a-days Finite Element Method is widely used in different fields of Geotechnical Engineering. So, such condition can also be applied for bearing capacity estimation. However, the accuracy of the FE analysis depends on the constitutive models of soils. Available constitutive models such as Cam clay model (Roscoe and Burland, 1968), Drucker-Prager Model, Mohr-Coloumb Model cannot properly consider or explain soil behavior of different densities. However, in this study extended sub-loading tij model [Nakai and Hinokio, 2004; Nakai , 2011] is used which can consider influence of intermediate principal stress on the deformation and strength of soils, dependence of the direction of plastic flow on the stress paths, influence of density and/or confining pressure and bonding effect on the deformation and strength of soils [Shahin, 2004; Nakai, 2010; Nakai, 2011].

2.2 Summary

From different research paper review we have come to know that in bearing capacity estimation sub-loading tij model for FEM analysis is very much convenient.

Chapter 3 Methodology

3.1 General

As the study has a wide insight on a variety of aspects, different methods were adopted in order to achieve the objective of this study properly. And by implementing these methods, a direct approach has been set out to fulfill the scope of the study. In this chapter, the methods adopted and implemented are discussed thoroughly.

3.2 Finite Element Modeling

The finite element program FEMtij-2D was used for evaluating the stability of embankment slope. The road embankment cross-section utilized for the numerical model is presented in figure 3.1

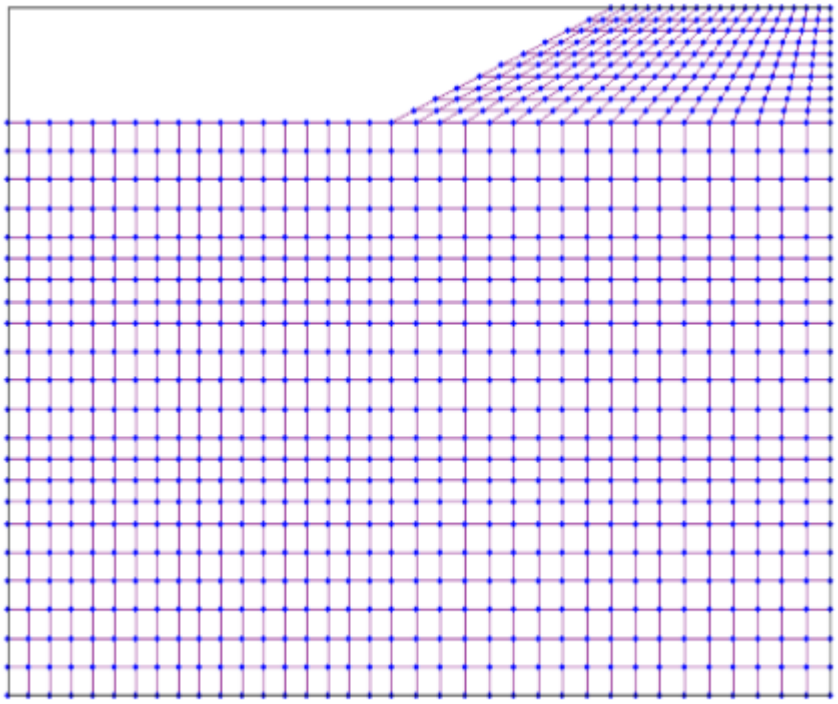

Figure 3.1: Left half of the embankment cross-section mesh

3.3 Mesh Generation and Boundary Conditions

In this modeling, 4-node rectangular elements were used; see figure 3.1. The powerful 4-node element provides an accurate calculation of stresses and failure loads. The two vertical boundaries are free to move vertically only supported as roller support at the left and right side of the embankment as shown in figure 3.2, whereas the horizontal boundary at the bottom is considered to be pinned support.

Chapter 3 Methodology

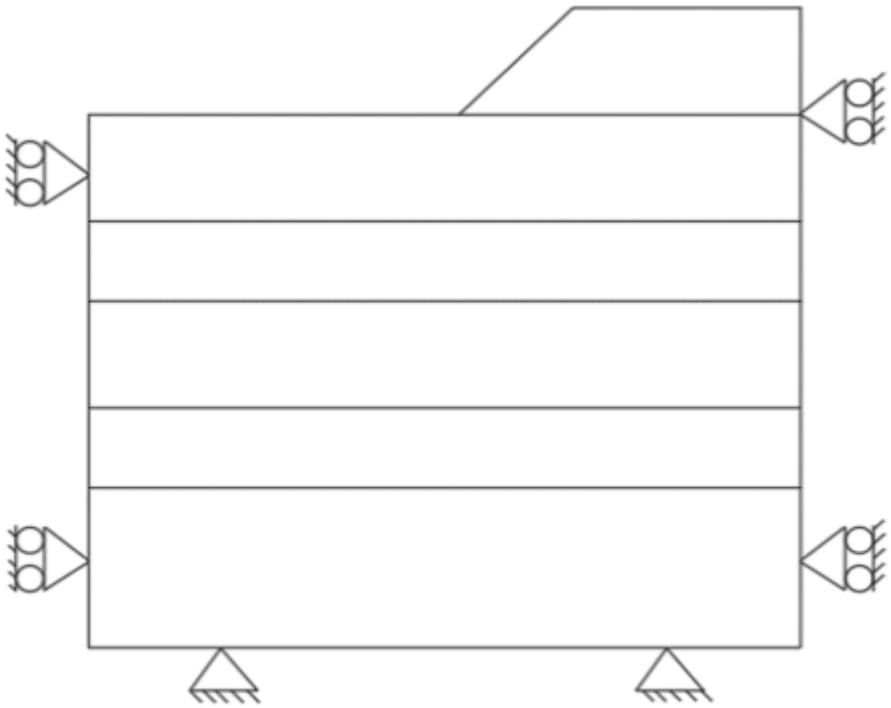

Figure 3.2: Boundary conditions used in analysis

3.4 Study Area

For the soil investigation, we have selected several places (figure 3.1) in Narayanganj (23.60°N to 90.50°E with an area of 683.14 km2) and Comilla (23.27°N to 91.12°E with an area of 3,146.30 km2) districts. In Narayanganj, we have collected soil from Sonargaon (23°38′51″N to 90°35′52″E with an area of 171.02 km2) and Bandar (23°37′N to 90°31.5′E with an area of 55.84 km2) upazilla. In Comilla, we have collected soil from Comilla Sadar Dakshin (23°22′N to 91°12′E with an area of 241.66 km2) and Chouddagram (23°13′N to 91°19′E with an area of 268.48 km2) upazilla. All these locations are shown in figure 3.1. In this study, the physical and geotechnical properties are carried out with the help of field observations and different laboratory tests.

Chapter 3 Methodology

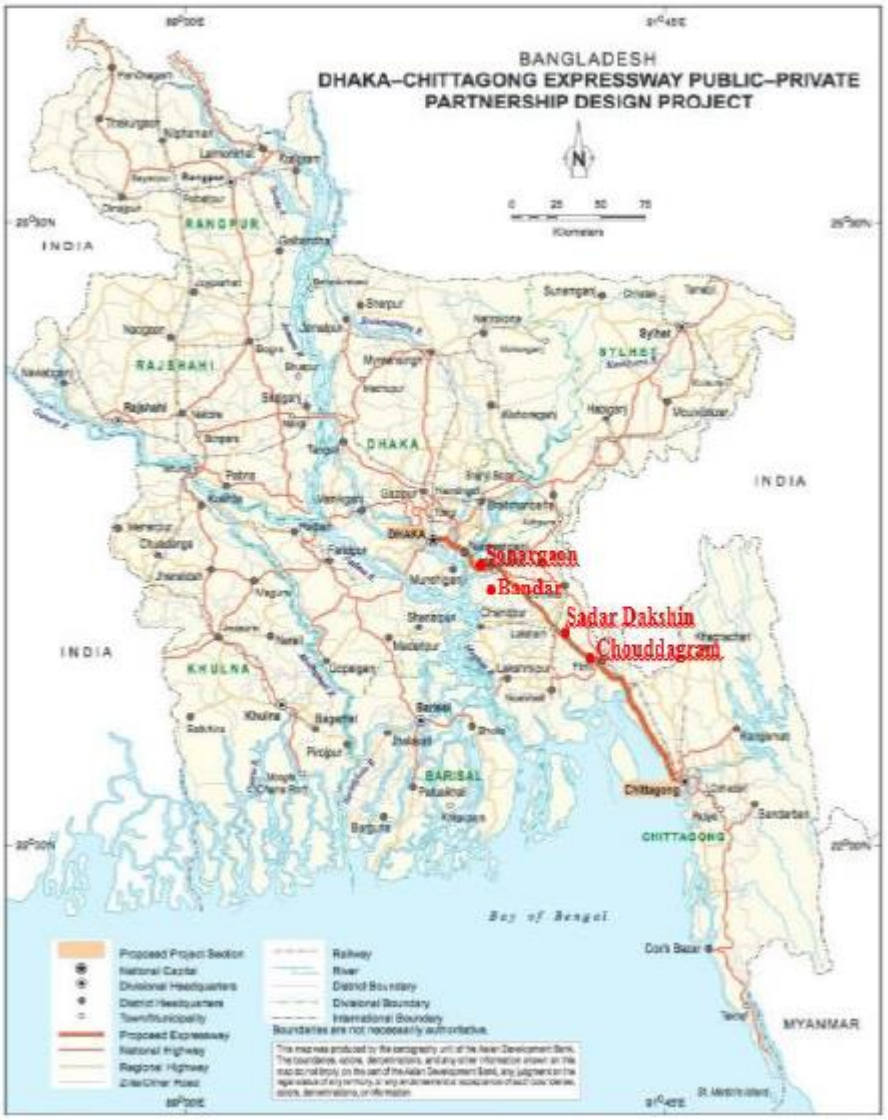

Fig 3.3 Proposed Dhaka-Chittagong elevated expressway

3.5 Material Collection

Soil samples are collected as boring sample using Shelby tubes. It is thin-walled open-tube samplers are designed for taking samples in soft and firm cohesive soils. These samplers have a much lower area ratio (approximately 10%) than U100 samplers and therefore give less disturbed samples. However, some disturbance is caused due to friction of the sample on the inside of the sample tube. Each tube has one end that is chamfered to form a cutting edge and the upper end includes holes for securing the tube to a drive head. Shelby tubes are useful for collecting soils that are particularly sensitive to sampling disturbance, including fine cohesive soils and clays. The tubes can also be used to transport samples back to the lab as well.

Figure 3.4. Shelby Tubes

So, the samples were undisturbed. The length of the each tube was 450 mm. We have collected samples from different depths of earth i.e. 5m, 10m, 15m, 20m and 30m below from the earth surface. These samples are then tested in laboratory by different experimental procedures.

Figure 3.5 Sample extraction from Shelby tube

3.6 Laboratory Experiments

We have performed several laboratory tests in the laboratory to determine various soil parameters. The tests we have performed are described briefly here.

3.6.1 Moisture Content of Soil

Water content or moisture content is the quantity of water contained in a material, such as soil (called soil moisture). We have determined moisture content of soil. We have followed procedure described below:

i) Clean the container, dry it and weigh it with the lid (Weight 'M_1').

ii) Take the required quantity of the wet soil specimen in the container and weigh it with lid(Weight 'M_2').

iii) Place the container, with its lid removed, in the oven till its weight becomes constant (Normally for 24hrs.).

iv) When the soil has dried, remove the container from the oven, using tongs.

v) Find the weight 'M_3' of the container with the lid and the dry soil sample.

Figure 3.6 Weight measurement of can

Chapter 3 Methodology

Water content or Moisture content of soil is measured to find out the quantity of water the soil sample has. We use the following formula to measure moisture content:

$$W_N = (\text{M2} - \text{M3} / \text{M3} - \text{M1}) * 100$$

An average of three determinations had been taken. The data we got is shown in Table 3.1.

Where,

W_n = Moisture content of soil (%)

M1 = Mass of empty can

M2 = Mass of wet soil + Can

M3 = Mass of dry soil + Can

Table 3.1: Moisture content measuring of soil sample

Moisture Content			
Can no.	43	66	54
can mass, g (M1)	28.90	26.60	34.30
Mass of wet soil + Can (M2)	53.90	56.60	69.30
Mass of dry soil + Can (M3)	48.10	49.50	61.10
Mass of dry soil, g (M3-M1)	19.20	22.90	26.80
Water content, %	30.21	31.00	30.60
Average		30.60	

A sample calculation :

Weight of water, M2-M3= 53.90-48.1=5.8

Weight of solid, M3-M1= 48.10-28.90=19.20

Water Content, Wn= (5.8/19.20)*100%=30.21%

3.6.2 Specific Gravity of Soil

Specific gravity (Gs) is defined as the ratio of the weight of an equal volume of distilled water at that temperature both weights taken in air. We have determined specific gravity of soil. We have followed procedure described below:

i) First we had cleaned and dried pycnometer. Then we had taken water into the pycnometer up to the mark and taken weight W1

ii) Then we had put the water out and taken 50 gm of oven dried soil in the pycnometer and took some water into it.

iii) Then we took the pycnometer and submerged it into boiling water and stirred it for 10 minutes. After 10 minutes we pulled the pycnometer out of water and kept it in rest to get cool down.

iv) After that we filled the pycnometer up to mark with water and taken weight W2. We have determined the water temperature and from chart we got specific gravity of water at that temperature.

v) Then from these value we calculated specific gravity three times and taken the average value.

Figure 3.7 Laboratory test of determination of Specific gravity of soil.

We have measured specific gravity (Gs) of soil samples (Table 3.2), to calculate the soil properties like Void Ratio (e0), Degree of Saturation etc. Data we collected during the test:

Table 3.2: Specific gravity measuring of soil sample

Determination No	1	2	3
Pycnometer No	1	2	3
Evaporating Dish No	15	10	28
Weight of dry Soil, w_s (gm)	50	50	50
Weight of Pycnometer + water (filled to the mark)= W_1 (gm)	352.92	353.82	355.92
Temperature of the Water, T^0 C	33	33	33
Weight of Pycnometer + Water (filled to the mark) + Soil= W_2	384.08	385.12	387.47
Weight of equal volume of water as the soil solids= W_w(gm)=(W_1+Ws)-W_2	18.84	18.7	18.45
Specific Gravity of Water= G_T at T^0 C	0.9957	0.9957	0.9957
Gs at T^0 C=(W_s/W_w) x G_T	2.64	2.66	2.70
Average specific gravity, G_s		2.67	

Sample Calculation:

Weight of dry Soil, ws = 50gm

Weight of Pycnometer + water (filled to the mark)= W1 = 352.92gm

Weight of Pycnometer + Water (filled to the mark) + Soil= W2 = 384.08gm

Weight of equal volume of water as the soil solids= Ww =(W1+Ws)-W2 =18.84gm

Specific Gravity of Water= GT = 0.9957

Specific gravity, Gs = (Ws/Ww)*GT = 2.64

3.4.3 Atterberg Limit of Soil

Liquid Limit is the minimum water content at which the soil is still in the liquid state, but has a small shearing strength against flow. The water content at which a soil will just begin to crumble when rolled into a thread approximately 1/8" (3 mm) in diameter. Plasticity index is the difference in moisture content of soils between the liquid and plastic limits expressed in percentage.

We have done Atterberg limit test to calculate Liquid Limit (LL) and Plastic Limit (PL) and Plasticity Index (PI) (Table 3.3) of the soil samples.

Variable	NO		Plastic Limit			Liquid Limit		
	Var.	Units	1	2	3	1	2	3
Number of Blows	N	blows				17	24	28
Can Number	---	---	12	53	47	66	65	51
Mass of Empty Can	M_C	(g)	34.36	32.83	24.84	26.62	29.21	29.17
Mass Can & Soil (Wet)	M_{CMS}	(g)	39.97	39.18	30.44	36.47	40.00	39.53
Mass Can & Soil (Dry)	M_{CDS}	(g)	38.60	37.63	29.05	33.71	37.09	36.83
Mass of Soil	M_S	(g)	4.24	4.80	4.21	7.09	7.88	7.66
Mass of Water	M_W	(g)	1.37	1.55	1.39	2.76	2.91	2.70
Water Content	w	(%)	32.3	32.3	33.0	38.9	36.9	35.2

Table 3.3: Atterberg limit measuring of soil sample

Chapter 3 Methodology

3.7 Layers of Soil Section with Piled Raft Foundation

From Figure 3.15 we can see a section of piled raft foundation with different layers o soil.

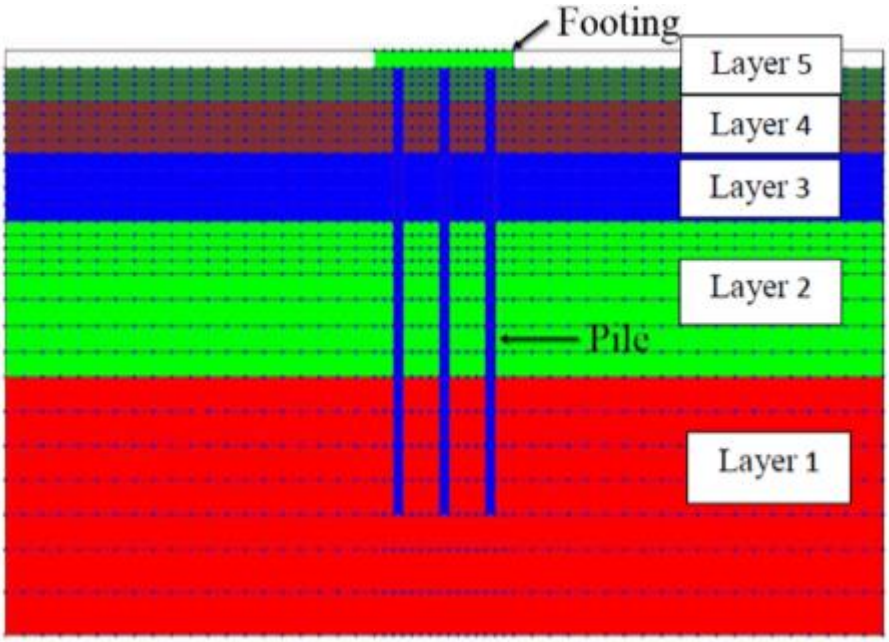

Fig 3.8 layers of piled raft foundation soil section

3.8 Mesh of Soil Section

Mesh generation is the practice of generating a polygonal or polyhedral mesh that approximates a geometric domain. The term "grid generation" is often used interchangeably. Typical uses are for rendering to a computer screen or for physical simulation such as finite element analysis or computational fluid dynamics.

Figure 3.16 is the mesh with dimension of the same section which has been done for simulation work.

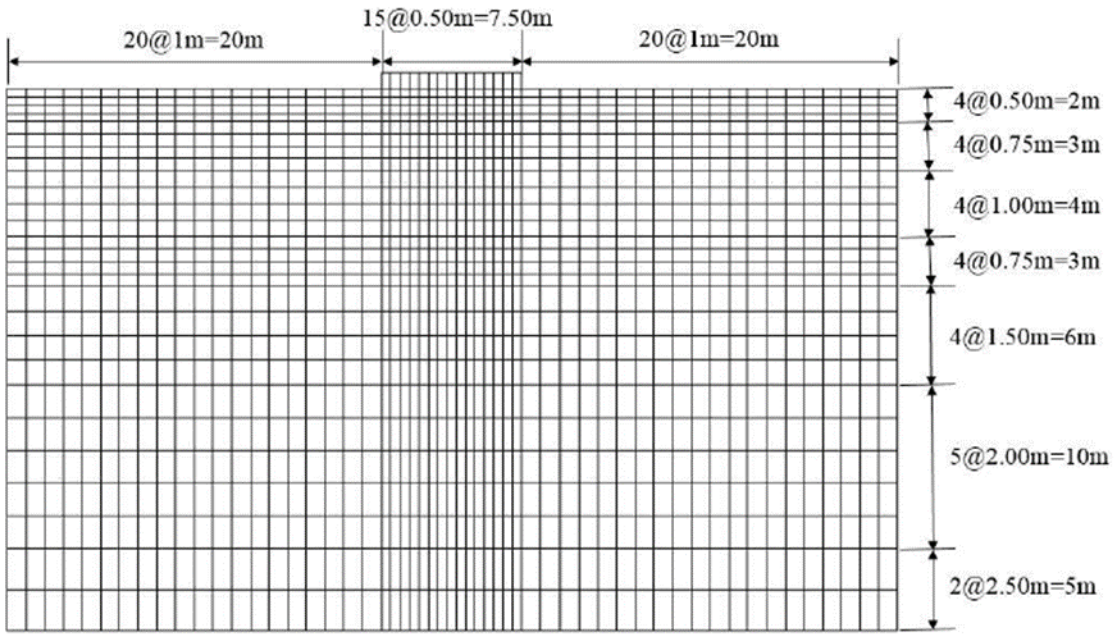

Figure 3.9. Finite Element Mesh for piled raft foundation

3.7 Conclusion

In this chapter, different methods adopted to achieve the objectives of the study are thoroughly discussed. Different parameters of soil are explained in order to relate it to the study result. Experimental method is important in order to set out the scope of the study. So, the methodology is followed by the result and discussion in the next cha

Chapter 4 Soil Characteristics at the Study Locations

Physically Narayanganj district is characterized by alluvial formations caused by several rivers such as Shitalakshya, Meghna, Old Brahmaputra, Buriganga, Balu and Dhaleshwari. Comilla district is mainly formed of olive grey silty loam and dark grey silty loam soil. By observing and testing we have found similarity among the soils of study locations in different depths which are shown in Figure 4.1.

Table 4.1: Simulation parameters

Soil Layers	Depth (m)	λ	ќ	β	RCs	N	e0	aAF	aIC
1	0.00-2.00	0.0700	0.00450	2.00	3.20	1.100	0.800	030	030
2	2.01-5.00	0.1038	0.00829	1.60	3.98	0.865	0.879	800	800
3	5.01-9.00	0.1018	0.00803	1.60	4.00	0.868	0.880	850	850
4	9.01-18.00	0.0819	0.00983	1.60	4.00	0.778	0.789	800	800
5	18.01-33.00	0.0879	0.00894	1.60	4.00	0.602	0.620	800	800

Chapter 4 Soil Characteristics at the Study Locations

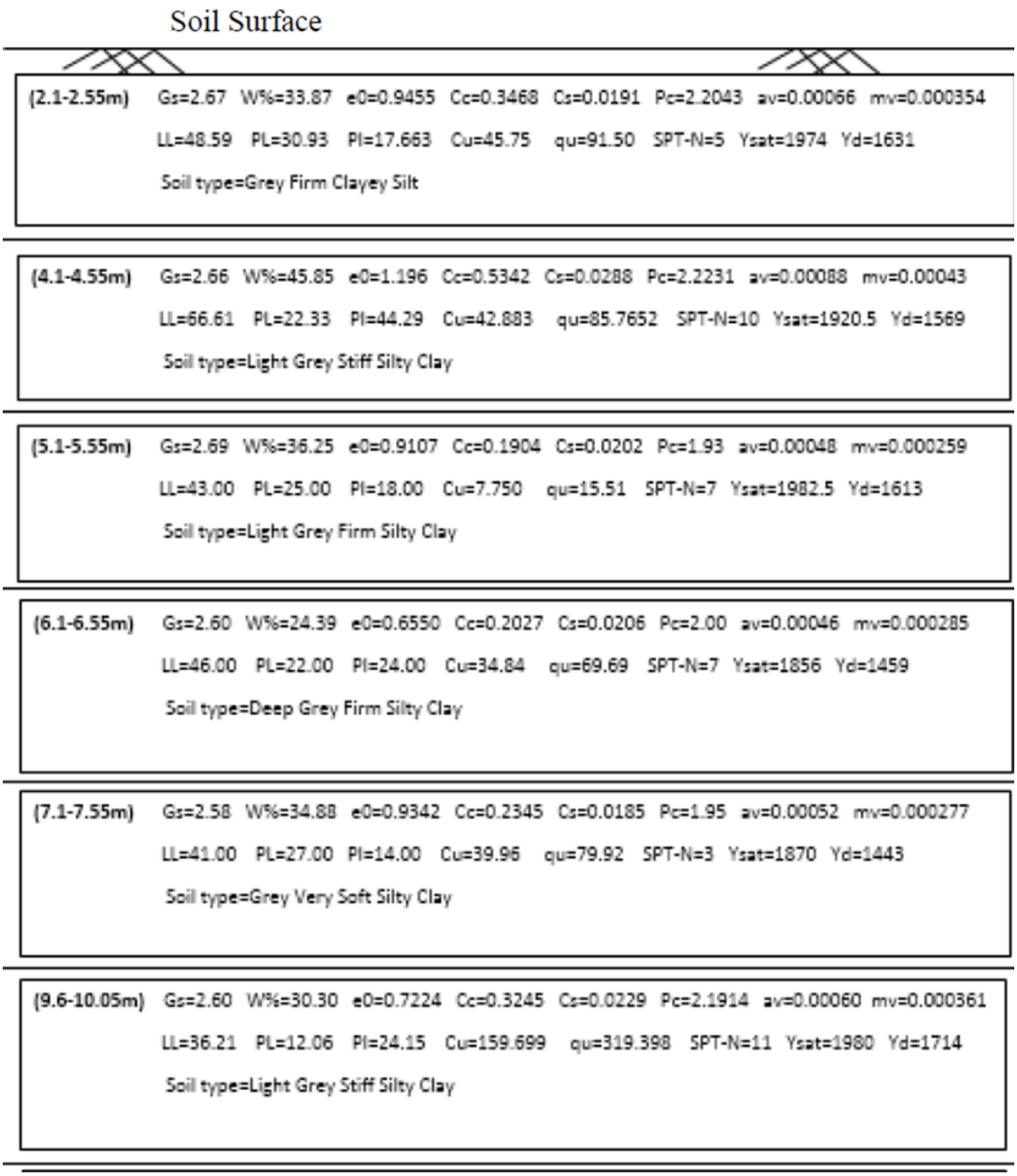

Figure 4.1. Soil parameters from laboratory tests

Chapter 5 Results and Discussions

5.1 General

This chapter deals with the presentation of results obtained from various tests and simulation conducted on soil. The main objective of the research program was to determine the bearing capacity of piled raft foundation.

5.2 Load Bearing Capacity

The bearing capacity of soils is perhaps the most important of all the topics in soil engineering. Soils behave in a complex manner when loaded so, it is important to know the bearing capacity of soils. Soil when stressed due to loading, tend to deform. The resistance to deformation of the soil depends upon factors like water content, bulk density, angle of internal friction and the manner in which load is applied on the soil. The maximum load per unit area which the soil or rock can carry without yielding or displacement is termed as the bearing capacity of soils.

5.3.1 Initial Stress Distribution of the Ground

Figure 5.4 shows the initial distribution of stress without piled raft foundation. Here we can see the stress in the deepest layer is highest.

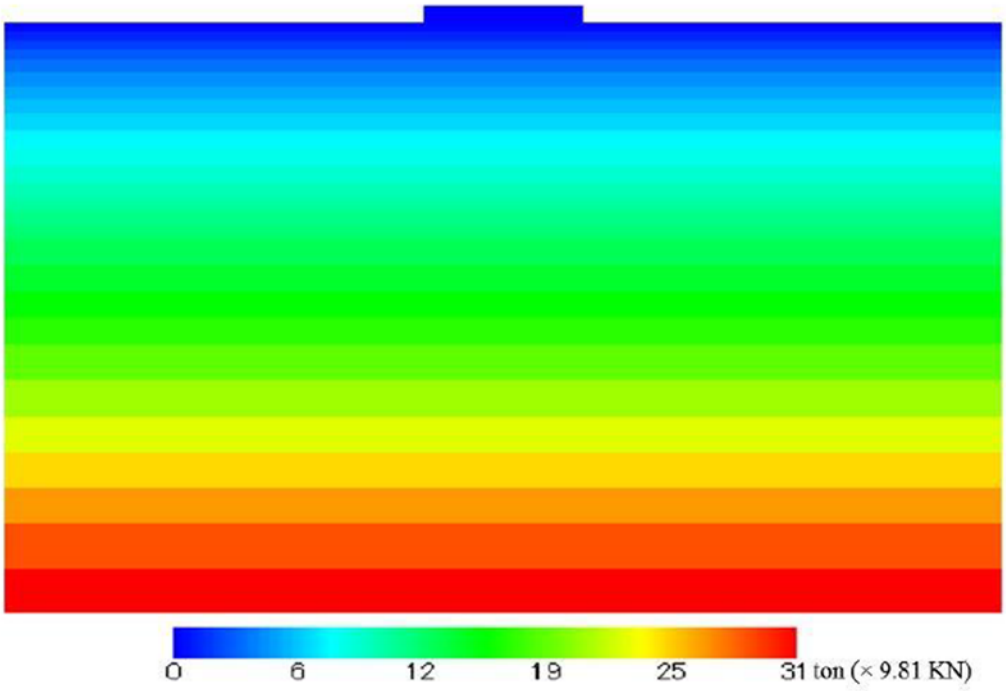

Figure 5.1 Stress distribution without piled raft foundation

5.3.2 Stress Distribution of the Groud with Structure Load

Figure 5.5 shows the initial distribution of stress with piled raft foundation. Here we can see hoe the piles are distributing the loads in the soil layer.

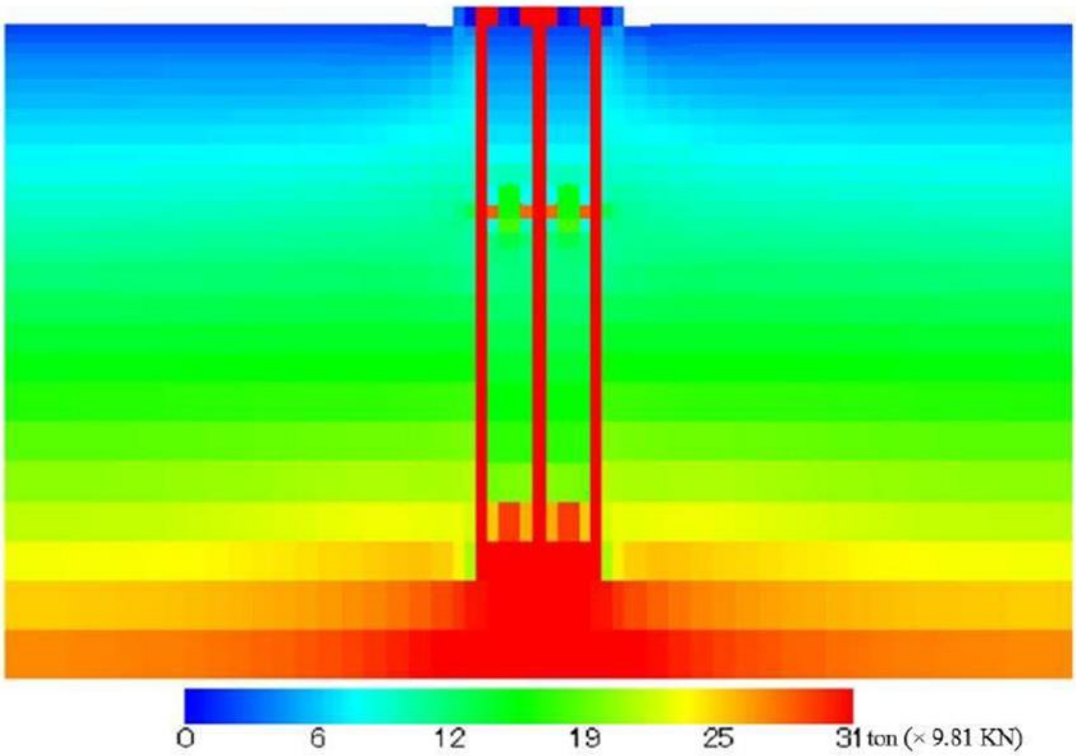

Figure 5.2 Stress distribution with piled raft foundation

5.3.3 Load-Displacement Relation

This the final result of our study through simulation. This figure 5.6 shows the nload bearing capacity of soil. For 0.05% settlement the soil can take 880 ton load.

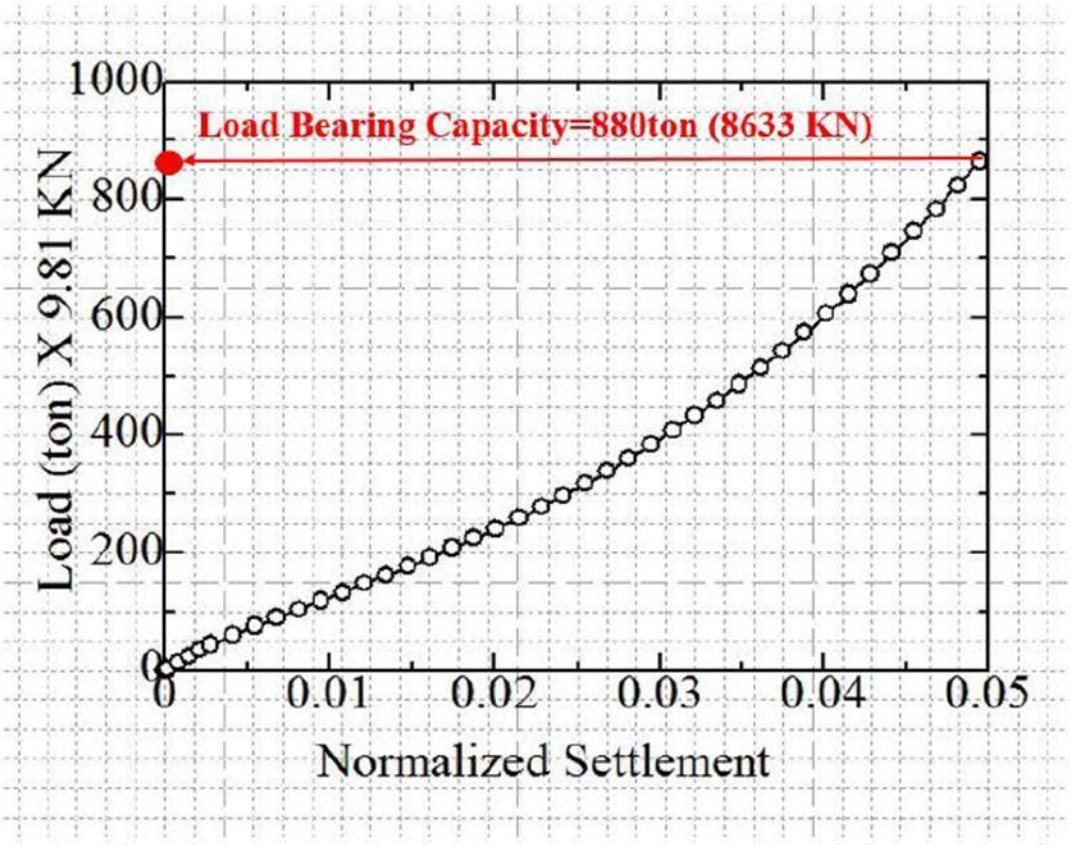

Figure 5.3 Load vs. Settlement curve

5.4 Vertical Stress Distribution in soil with pile length decreased

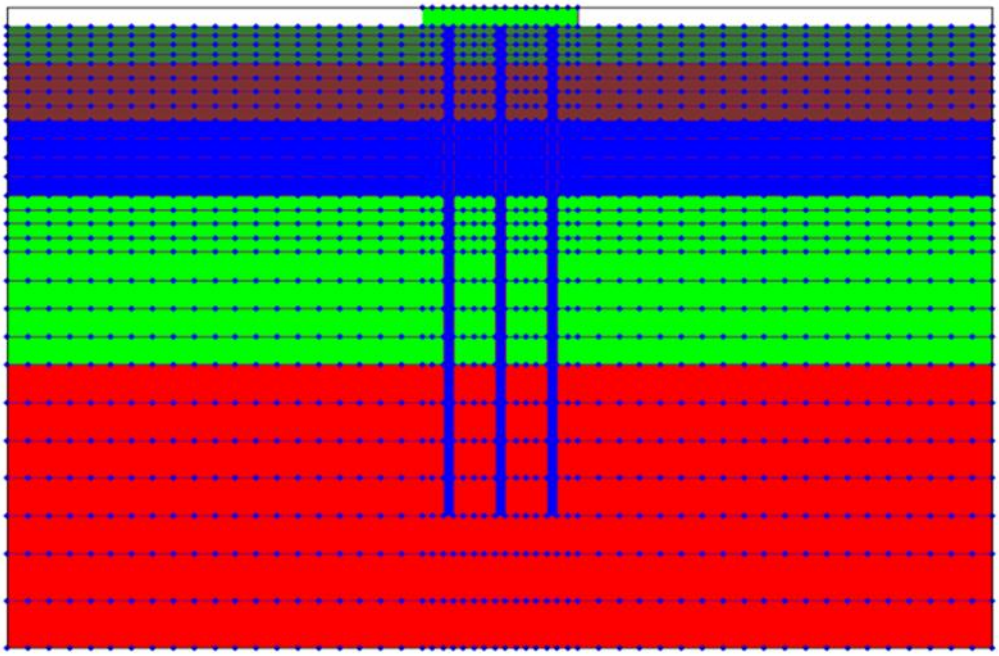

Fig 5.4 Layers of pile raft foundation

5.5 Stress distribution in Pile raft after 500 steps

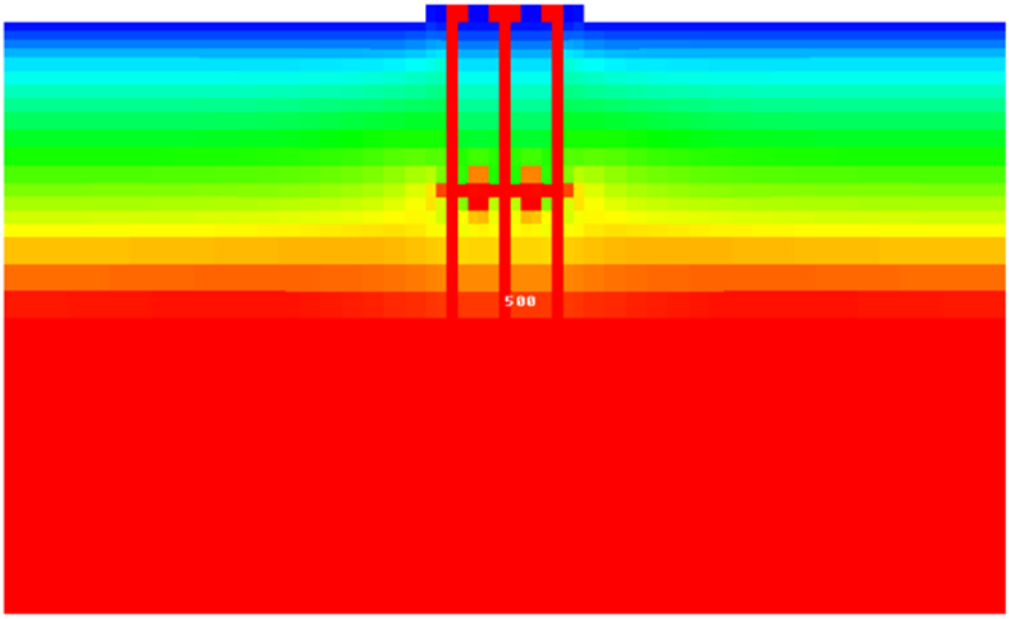

Fig 5.5 Stress distribution in Pile raft after 500 steps

Chapter 5 Results and Discussions

5.6 Stress distribution in soil after 2500 steps

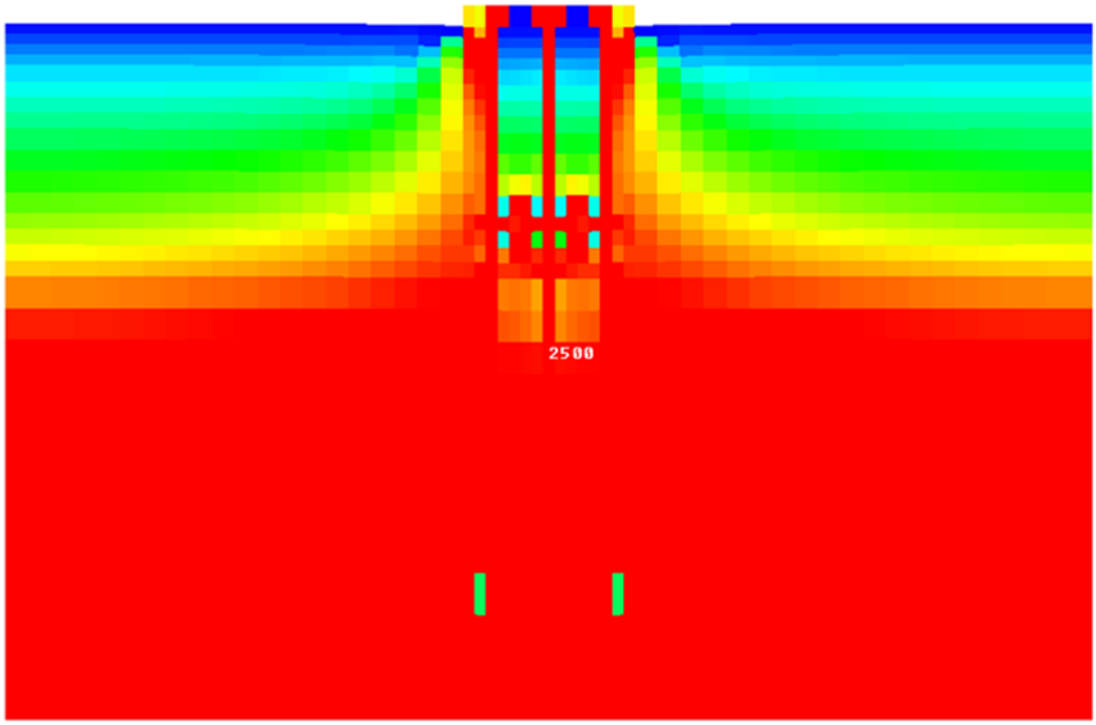

Fig 5.6 Stress distribution in Pile raft after 2500 steps

5.7 Stress distribution in soil after 10000 steps

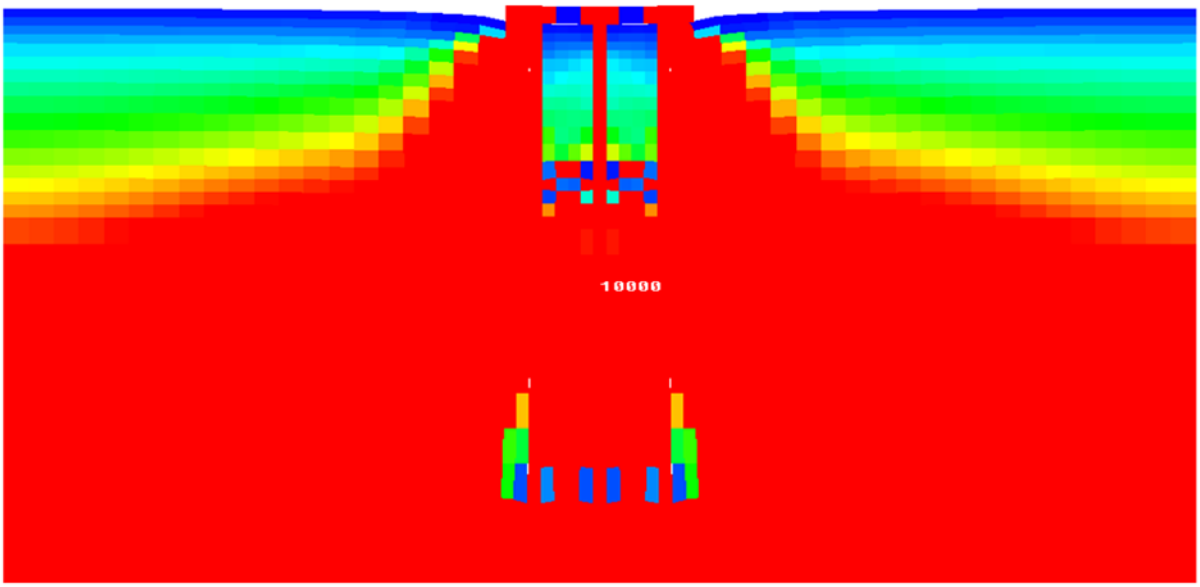

Fig 5.7 Stress distribution in soil after 10000 steps

Chapter 6 Conclusion

6.1 Reviews on Completed Research Work

6.1.1 Load Bearing Capacity

Load bearing capacity for 0.05% vertical settlement of soil = 880 ton or 8633KN.

- The vertical stress in soil is significantly more with pile length decreased.
- Increased Pile Length shows more bearing capacity
- The Bearing Capacity was higher for Increased Pile length in our simulations

6.2 Future Research

Calculation of ultimate bearing capacity of piled raft foundation and pile foundation varying-

- Number of piles
- Length of piles
- Diameter of piles
- Changing the height of the water table

References

Azzouz, A.S., Krizek, R.J., Corotis,R.B., (1976). Regression analysis of soil compressibility. Soils Foundation 16(2), 19–29

Cozzolino, V.M. (1961). Statistical forecasting of compression index. Proceedings of the Fifth International Conference on Soil Mechanics and Foundation Engineering, Paris, vol.1, pp.51–53

Danial Mohammadzadeh S., Jafar Bolouri Bazaz, AmirH.Alavi, (2014). An evolutionary computational approach for formulation of compression index of fine- grained soils. Engineering Applications of Artificial Intelligence, 33(2014), 58–68

Kazimierz Józefiaka, Artur Zbiciaka, Maciej Maslakowski, Tomasz Piotrowskib, (2015). Numerical modelling and bearing capacity analysis of pile foundation. XXIV R-S-P seminar, Theoretical Foundation of Civil Engineering (24RSP) (TFoCE 2015), Procedia Engineering 111 (2015), 356 – 363

Mayne, P.W., (1980). Cam-clay predictions of undrained strength. J.Geotech. Eng. Div. ASCE 106(11), 1219–1242

Mohammad S. Islam, H.M. Shahin, S. Banik, F. Azam (2013). Elasto-plastic constitutive model parameters and their application to bearing capacity estimation for Dhaka sub-soil. Journal of Civil Engineering (IEB), 42 (2), 171-188

Nakai, T. and Hinokio, T. (2004). A simple elastoplastic model for normally and over consolidated soils with unified material parameters, Soils and Foundations, 44(2), 53- 70

References

Nakai, T., Shahin, H.M., Zhang, F. Hinokio,M., Kikumoto, M., Onaha, S. and Nishio, A. (2010). Bearing capacity of reinforced foundation subjected to pull-out loading in 2D and 3D conditions. Geotextiles and Geomembranes, 28(3), 268-280

Nakai, T. Shahin, H.M., Kikumoto, M., Kyokawa, H., Zhang, F.and Farias, M.M. (2011). A simple and unified three-dimensional model to describe various characteristics of soils. Soils and Foundations, 51(6), 1149-1168

Nishida. Y., (1956). A brief note on compression index of soils. J. Soil Mech. Found. Div., ASCE 82 (SM3) (1027-1-1027-14)

Park,H., Lee,S.R., (2011). Evaluation of the compression index of soils using an artificial neural network. Comput.Geotech.38, 472–481

Roscoe, K. H. and Burland, J. B. (1968). On the generalized stress-strain behaviour of wet clay. Engineering Plasticity, Cambridge: 535-609

Skempton, A.W. (1944). Notes on the compressibility of clays. Quart. J.Geol. Soc.

Lond. 100, 119–135

Sower, G.B., (1970). Introductory Soil Mechanics and Foundation, 3rd Ed. The Macmillan Company of Collier-Macmillan Ltd, London

Terzaghi, K., Peck, R.B., (1967). Soil Mechanics in Engineering Practice. John Wiley & Sons Inc., New York.

T.W. Lambe, R.V. Whitman, Soil Mechanics, Wiley, New York, 1969

Wroth,C.P., Wood,D.M., (1978). The correlation of index properties with some basic engineering properties of soils. Can.Geotech.J. 15, 137–145

APPENDIX

REVIEW OF THE EXTENDED SUBLOADING t_{ij} MODEL

This model, despite the use of a small number of material parameters, can describe properly the following typical features of soil behaviors (Nakai and Hinokio, 2004 & Nakai et al., 2011):

(i) Influence of intermediate principal stress on the deformation and strength of geomaterials.

(ii) Dependence of the direction of plastic flow on the stress paths.

(iii) Influence of density and/or confining pressure on the deformation and strength of geomaterials.

(iv) The behavior of structured soils such as naturally deposited soils.

A brief description of the above mentioned features of this model can be made as follows:

Influence of intermediate principal stress is considered by defining yield function f with modified stress t_{ij} (i.e., defining the yield function with the stress invariants (t_N and t_S) instead of (p and q) and considering associate flow rule in t_{ij} –space instead of σ_{ij} –space (Nakai and Mihara (1984)). The stress and strain increment tensors and their parameters using ordinary concept and t_{ij}-concept are compared in Table 2. As shown in Fig. 6, the stress tensors and parameters in the ordinary models are defined as the quantities related to normal and parallel components of σ_{ij} to the octahedral plane. On the other hand, as shown in Fig. 7, the stress tensors and stress parameters of the t_{ij}-concept are those of normal and parallel components of the modified stress t_{ij} to the spatially mobilized plane (briefly SMP; Matsuoka and Nakai (1974)).

Figure 8(a) shows the yield surfaces of an elastoplastic model based on the t_{ij} concept, represented on the $t_N - t_S$ plane, in which the direction of plastic values are assigned as the direction cosines of the Specially Mobilized Plane according to the following equation (Nakai (1989)).

$$a_i = \sqrt{\frac{I_3}{I_2 \sigma_i}} \quad (i = 1,2,3) \qquad (1)$$

where σ_i (i=1,2,3) are the three principal stresses, I_2, and I_3 are the second and third invariants of σ_{ij}, The principal axes of t_{ij} coincide with those of σ_{ij}, because the principal axes of a_{ij} and σ_{ij} are identical.

According to subloading surface concept, yield surface (subloading surface) has not only to expand but also to shrink for the present stress state to lie always on the surface, and the yield function is written as a function of the mean stress t_N and stress ratio $X \equiv t_S / t_N$ based on t_{ij} by Eq.(2).

$$F = H \text{ or } f = F - H = 0 \qquad (2)$$

Where, $F = (\lambda - \kappa) \ln \frac{t_{N1}}{t_{N0}} = (\lambda - \kappa) \left\{ \ln \frac{t_N}{t_{N0}} + \varsigma(X) \right\}$ and $H = \left(-\Delta e\right)^p = (1 + e_0) \cdot \varepsilon_v^p$

Here, t_{N1} determines the size of the yield surface (the value of t_N at X=0), t_{N0} is the value of t_N at reference state. The symbols λ and κ denote compression index and swelling index, respectively, and e_0 is the void ratio at reference state. $\varsigma(X)$ is an increasing function of stress ratio $X(=t_S/t_N)$ which satisfies the condition $\varsigma(0)=0$. In this research, the expression for $\varsigma(X)$ is assumed as,

$$\varsigma\left(X\right) = \frac{1}{\beta}\left(\frac{X}{\mathrm{M}^*}\right)^{\beta} \quad (\square : \text{material parameter}) \quad (3)$$

The value of M* in Eq.(3) is expressed as follows using principal stress ratio $X_{CS} \equiv (t_S/t_N)_{CS}$ and plastic strain increment ratio $Y_{CS} \equiv (d\varepsilon_{SMP}^{*p} / d\gamma_{SMP}^{*p})_{CS}$ at critical state:

$$\mathrm{M}^* = \left(X_{CS} + X_{CS}^{\beta - 1} Y_{CS} \right)^{1/\beta} \qquad (4)$$

and these ratios X_{CS} and Y_{CS} are represented by the principal stress ratio at critical state in triaxial compression R_{CS}:

$$X_{CS} = \frac{\sqrt{2}}{3}\left(\sqrt{R_{CS}} - \frac{1}{\sqrt{R_{CS}}}\right) \quad (5)$$

$$Y_{CS} = \frac{1-\sqrt{R_{CS}}}{\sqrt{2}\left(\sqrt{R_{CS}}+0.5\right)} \quad (6)$$

In elastoplastic theory, total strain increment consists of elastic and plastic strain increments as

$$d\varepsilon_{ij} = d\varepsilon_{ij}^{e} + d\varepsilon_{ij}^{p} \quad (7)$$

Here, plastic strain increment is divided into component $d\varepsilon_{ij}^{p(AF)}$, which satisfies associate flow rule in the space of modified stress t_{ij}, and isotropic compression component $d\varepsilon_{ij}^{p(IC)}$as given in Eq.(8).

$$d\varepsilon_{ij}^{p} = d\varepsilon_{ij}^{p(AF)} + d\varepsilon_{ij}^{p(IC)} \quad (8)$$

The components of strain increment are expressed as,

$$d\varepsilon_{ij}^{p(AF)} = \Lambda \frac{\partial F}{\partial t_{ij}} \quad (9)$$

$$d\varepsilon_{ij}^{p(IC)} = \Lambda^{(IC)} \frac{\delta_{ij}}{3} \quad (10)$$

Here, Λ is the proportionality constant, δ_{ij} is Kronecker's delta. Dividing plastic strain increment into two components as in Eqs.(8) to (10), for the same yield function, this model can take into consideration feature (ii), i.e., the dependence of the direction of plastic flow on the stress paths.

Referring to the subloading surface concept by Hashiguchi (1980) and revising it, i.e., adding the term $G(\rho)$ in the denominator of the proportionality constant Λ of normal

consolidated condition, influence of density is considered. In the modeling based on the subloading surface concept (Hashiguchi, 1980), it is assumed that the current stress point always passes over the yield surface (subloading surface) whether plastic deformation occurs or not. The proportionality constant Λ is expressed as

$$\Lambda = \frac{\dfrac{\partial F}{\partial \sigma_{ij}} d\sigma_{ij} - \dfrac{\lambda - \kappa}{t_{N1}} \langle dt_N \rangle}{(1+e_0)\left(\dfrac{\partial F}{\partial t_{kk}} + \dfrac{G(\rho)}{t_N} \right)} = \left(\frac{\dfrac{\partial F}{\partial \sigma_{ij}} D^e_{ijkl} d\varepsilon_{kl}}{h_p + \dfrac{\partial F}{\partial \sigma_{mn}} D^e_{mnop} \dfrac{\partial F}{\partial t_{op}}} \right) \quad (11)$$

and

$$\Lambda^{(IC)} = \frac{\dfrac{\lambda - \kappa}{t_{N1}} \langle dt_N \rangle}{(1+e_0)\left(1 + \dfrac{G(\rho)}{(\lambda - \kappa) a_{kk}} \right)} \quad (12)$$

Here, the symbol < > denotes Macauley bracket.

As shown in Figure 8(b), the initial and current void ratios for over consolidated soils are expressed as e_0 and e and the state variable □□which represents the influence of density is defined as □=e_N-e and its initial value is (□□=e_{N0}-e_0). In the definition of Λ as in Eq.(11), ρ decreases with the development of plastic deformation and eventually becomes zero. To satisfy this condition, $G(\rho)$ should be a increasing function of ρ which satisfies $G(0) = 0$, such as

$G(\rho) = sign(\rho) a \rho^2$ (a: material parameter) (13)

The evolution rule of ρ is given as

$$d\rho = -(1+e_0) \frac{G(\rho)}{t_N} \Lambda \quad (14)$$

In feature (iv), the stress-strain behavior of structured soil can be described by considering not only the effect of density described above but also the effect of bonding. Two state

variables ρ related to density and ω representing the bonding effect are used to consider feature (iv). Here, the evolution rule of □ is then given as

$$d\rho = -(1+e_0)\left\{\frac{G(\rho)}{t_N} + \frac{Q(\omega)}{t_N}\right\}\Lambda \qquad (15)$$

The evolution rule of ω is given as

$$d\omega = -(1+e_0)\frac{Q(\omega)}{t_N}\Lambda \qquad (16)$$

In the present model, the following linear increasing function $Q(\omega)$ is adopted:

$$Q(\omega) = b\omega \qquad (17)$$

Finally, the proportionality constant Λ is expressed as:

$$\Lambda = \frac{\frac{\partial F}{\partial \sigma_{ij}} d\sigma_{ij}}{(1+e_0)\left(\frac{\partial F}{\partial t_{kk}} + \frac{G(\rho)}{t_N} + \frac{Q(\omega)}{t_N}\right)} = \frac{dF}{h^p} \qquad (18)$$

The loading condition of soil through its hardening process to softening process is presented as follows:

$$\begin{cases} d\varepsilon_{ij}^p \neq 0 & if \quad \Lambda = \dfrac{dF}{h^p} \geq 0 \\ d\varepsilon_{ij}^p = 0 & otherwise \end{cases} \qquad (19)$$